A Bacteriolysin of Lactococcus carnosus is potentially involved in mediating contact-dependent antagonism against Listeria monocytogenes

Raouf Tareb
Oniris, INRAE, SECALIM
Sandrine Rezé
Oniris, INRAE, SECALIM
Manar Harb
Oniris, INRAE, SECALIM
Laurence Dubreil
Oniris, INRAE, APEX
Veronique Monnet
PAPPSO, Micalis Institute, Université Paris-Saclay
Joanna Björkroth
Department of Food Hygiene and Environmental Health, Faculty of Veterinary Medicine, University of Helsinki, Helsinki, Finland
Delphine Passerini
Ifremer, MASAE
Francoise Leroi
Ifremer, MASAE
Marie-France Pilet
marie-france.pilet@inrae.fr

Oniris, INRAE, SECALIM

Article

Keywords: Lactic Acid Bacteria, contact-dependent inhibition, bacteriolysin, peptidoglycan hydrolase, anti-listeria

Posted Date: October 30th, 2024

DOI: https://doi.org/10.21203/rs.3.rs-5261958/v1

Additional Declarations: No competing interests reported.

Article Title: A Bacteriolysin of *Lactococcus carnosus* is potentially involved in mediating contact-dependent antagonism against *Listeria monocytogenes*

Raouf Tareb[1], Sandrine Rezé [1], Manar Harb[1], Laurence Dubreil[2], Veronique Monnet[3], Joanna Björkroth[4], Delphine Passerini[5], Francoise Leroi[5], Marie-France Pilet[1*].

[1] Oniris, INRAE, SECALIM, Nantes, France
[2] Oniris, INRAE, APEX, PAnTher, Nantes, France
[3] PAPPSO, Micalis Institute, INRAE, AgroParisTech, Université Paris-Saclay, Jouy-en-Josas, France
[4] Department of Food Hygiene and Environmental Health, Faculty of Veterinary Medicine, University of Helsinki, Helsinki, Finland
[5] Ifremer, MASAE, Nantes, France

*Corresponding author

Abstract

Lactococcus carnosus CNCM I-4031 is a psychrotrophic lactic acid bacterium used for the biopreservation of seafood. It effectively inhibits the growth of spoilage and pathogenic bacteria, such as *Listeria monocytogenes,* through an atypical mechanism that relies on direct cell-to-cell contact, without producing conventional antimicrobial compounds like bacteriocins. However, the precise molecular mechanism behind this bacterial interaction remains to be fully understood. In this study, Label-free LC-MS/MS shotgun proteomics and gene expression analysis were used to examine cell envelope protein expression in *L. carnosus* when cultivated alone and in co-culture with *L. monocytogenes*. The investigation identified a specific cell wall protein, named LYSO, which has a toxic C-terminal domain and demonstrates peptidoglycan hydrolysis activity against L. monocytogenes. Further analysis using knockout mutants provided additional evidence for the involvement of LYSO in the inhibition activity. These findings suggest the significant role of this bacteriolysin in the contact-dependent mechanism of *L. carnosus against L. monocytogenes.*

Keywords: Lactic Acid Bacteria, contact-dependent inhibition, bacteriolysin, peptidoglycan hydrolase, anti-*listeria.*

29 **Introduction**

30 Bacterial ecosystems within food are highly diverse, featuring an array of microorganisms, including
31 spoilage bacteria, foodborne pathogens, and those contributing positively to product quality. When
32 different strains of bacteria coexist in the same environment, their interactions can lead to various
33 outcomes, such as neutralism, commensalism, mutualism, amensalism, and competition [1]. These
34 interactions have significant implications for the overall quality of food products. Notably, amensalism,
35 which refers to the suppression of one bacterial species by another without any reciprocal effect, has
36 received extensive attention in the study of Lactic Acid Bacteria (LAB) to identify strains with
37 significant potential in inhibiting unwanted spoilage bacteria and foodborne pathogens across various
38 food products[2].

39 *Listeria monocytogenes* is of particular concern among foodborne pathogens due to its ability to
40 withstand challenging conditions in the food production chain and cause listeriosis, one of the most
41 severe foodborne diseases[3]. This ubiquitous pathogen has been isolated from a large variety of
42 foodstuffs and is particularly of concern in ready-to-eat food. *L. monocytogenes* is a major risk for the
43 consumers and the food industry with an alarming mortality rate (20%–30%) for infected humans [3,4] .
44 Consequently, there has been a growing focus on biologically milder and healthier food preservation
45 approaches to control this pathogen.

46 One promising method is the use of LAB as bioprotective agent, which have demonstrated substantial
47 potential in enhancing food safety and stability[5]. However, for effective application of LAB, it is crucial
48 to understand their interaction mechanisms with target microorganisms. This understanding must
49 consider both biotic and abiotic factors associated with the food matrix, as well as the production and
50 preservation processes[6]. Historically, the inhibitory mechanisms of LAB have been primarily
51 associated with nutritional competition and the production of diffusible organic acids and bacteriocins

52 [7,8]. Bacteriocins, a specific class of antimicrobial peptides, are released by bacteria and act from a
53 distance to harm susceptible cells, providing a competitive advantage to the producing bacteria [9,10]. By
54 comprehensively understanding these mechanisms, we can optimize the efficiency of LAB as
55 bioprotective agents, ensuring safer and more stable food products.

56 *Lactococcus* CNCM I-4031, renamed *Lactococcus carnosus* CNCM I-4031[11], a psychrotrophic lactic
57 acid bacterium, has emerged as a promising bioprotective strain for seafood products[12,13]. This strain
58 has demonstrated the ability to improve cooked shrimp's sensory quality and microbial safety by
59 inhibiting the growth of *Brochothrix thermosphacta*[14] and *L. monocytogenes* [15], respectively. Recent
60 studies have highlighted the competitiveness of *L. carnosus* strains and their capacity to significantly
61 reduce the growth of various spoilage and foodborne pathogenic bacteria, including gram-negative and
62 gram-positive species[16]. However, the antimicrobial mechanism employed by *L. carnosus* against
63 different pathogens and spoilage organisms still need to be fully understood. Notably, recent research
64 has revealed that the inhibitory effect of *L. carnosus* CNCM I-4031 on *L. monocytogenes* is not
65 mediated by the release of diffusible antimicrobial compounds (such as known bacteriocins) or
66 nutritional competition, as commonly observed in LAB interactions. Instead, it depends on direct cell-
67 to-cell contact [17].

68 Contact-dependent growth inhibition occurs when a bacterial cell transfers a polymorphic toxin
69 molecule into neighbouring bacterial cells. Previous research has shed light on Gram-negative
70 bacteria's ability to efficiently deliver various antimicrobial toxins to closely related or genetically
71 distinct bacterial species through direct cell-to-cell contact [18]. This delivery of antimicrobial toxins is
72 often facilitated by specialized secretion systems (SS) such as Type 1SS, Type 4SS, Type 6SS, and
73 contact dependant inhibition (CDI) systems [9,10,18–21]. In contrast, there has been relatively limited
74 research exploring the capacity of gram-positive bacteria to deploy interspecies toxins through direct

75 cell-to-cell contact. Nonetheless, instances of such interactions have been documented in bacteria such
76 as *Bacillus subtilis*, *Bacillus megaterium*, *Streptococcus intermedius*, and *L. monocytogenes* [22–25].

77 This study aims to explore the contact-dependent growth inhibition observed in *L. carnosus* CNCM I-
78 4031 by elucidating its molecular mechanism. To achieve this, we will conduct a comprehensive
79 investigation using label-free LC-MS/MS shotgun proteomics and relative gene expression analysis.
80 In this work, we have investigated the expression of cell envelope proteins in *L. carnosus* CNCM I-
81 4031, both when cultivated in monoculture and when cocultured in contact with *L. monocytogenes*.
82 The analysis enables to identify a significant candidate among the cell wall proteins of *L. carnosus*
83 CNCM I-4031, a putative peptidoglycan hydrolase named LYSO. Further analysis indicates that LYSO
84 exhibits a toxic C-terminal domain and displays peptidoglycan hydrolysis activity against *L.*
85 *monocytogenes*. Additionally, the characterization of a knockout mutant of the LYSO protein suggests
86 its involvement in the contact-dependent growth inhibition of *L. monocytogenes* by *L. carnosus* CNCM
87 I-4031.

88 **Results**

89 **Identification of differentially abundant proteins of *L. carnosus* CNCM I-4031 in the coculture**
90 **with *L. monocytogenes* relative to the monoculture condition**

91 This study used a proteomic approach to investigate the cell-to-cell contact inhibition mechanism of *L.*
92 *monocytogenes ScottA* by *L. carnosus* CNCM I-4031. Specifically, we extracted and analyzed cell
93 envelope protein-enriched fractions from three biological replicates of the coculture of *L. carnosus*
94 CNCM I-4031 in contact with *L. monocytogenes ScottA* and compared these with the monoculture of
95 *L. carnosus*. Our analysis revealed 911 proteins for *L. carnosus* CNCM I-4031 under monoculture
96 conditions and 934 under coculture conditions (Fig. S1 and Supplemental file 1). Of these, 780 and
97 820 proteins were shared in all three biological experiments in monoculture and coculture conditions,
98 respectively (Fig. S1A–B).

99 Moreover, mutual exclusivity analysis revealed that 737 proteins were shared to both culture
100 conditions, while 43 and 83 proteins were specific to the monoculture and coculture conditions,
101 respectively (Fig. S1C). Thus, 863 proteins were identified in both coculture and monoculture
102 conditions, representing 43 % of the predicted ORFs encoded by the *L. carnosus* CNCM I-4031
103 genome (Table S1). Supplementary Table S1 overviews the predicted localizations of the 863
104 recovered proteins from *L. carnosus* CNCM I-4031 in both culture conditions. According to the
105 LocateP prediction, 693 (44%) were identified as cytoplasmic proteins, and 170 were predicted to have
106 a cell envelope localization. Among the cell envelope proteins, 85 were integral membrane proteins,
107 and 85 were surface proteins. The results demonstrated notable representation compared to the
108 expected envelope-proteins in the *L. carnosus* CNCM I-4031 genome. After analysis of each
109 independent biological replicate, a final dataset containing only proteins present in all three datasets
110 was generated (Suppl file 1).

111 To identify differentially abundant proteins between the two experimental conditions, our analysis
112 focused on protein candidates that met stringent criteria, requiring a minimum of two peptides and
113 consistent detection in all three biological replicates. This selection ensured a reliable dataset for
114 subsequent analyses. Besides, the samples from each replicate demonstrated robust technical and
115 biological reproducibility, as evidenced by calculating high Pearson correlation coefficients and
116 hierarchical analysis of spectral counts across the comprehensive set of proteins identified in both
117 culture conditions. The results of these analyses are depicted in Supplementary Figure S2, further
118 validating the consistency and reliability of our experimental approach. Based on a set of statistical
119 criteria (T-test p-value < 0.05 and Log2 "fold change" cutoff point > 2), we highlighted 42 proteins
120 with significantly changed abundance between the two conditions (Fig. 1 A-B and Supplemental file
121 1). Among these proteins, 27 were significantly more abundant (MA), and 15 were less abundant (LA)
122 in coculture conditions. Regarding the subcellular localization of the 27 MA proteins found in coculture
123 conditions (Table 1), 19 were predicted to have a cytoplasmic localization, and 5 were identified as
124 cell envelope proteins. Among the cell envelope proteins, 3 were predicted to be integral membrane
125 proteins, and 2 were cell surface-exposed proteins (LYSO: SCA91560.1 and PLY: SCA91317.1). The
126 MA proteins were categorized into biological process categories as defined by GO AND KEGG
127 databases (Table 1). They were mainly classified into various functional groups, including amino acid
128 (4), purine (3), lipid (3), and carbohydrate (3) transport and metabolism. The remaining identified
129 proteins were categorized as transcriptional regulators (4), proteins of unknown function (4) or
130 associated with DNA recombination and repair (3), and plasmid replication and mobilization (3). Of
131 particular interest, two cell surface-exposed proteins (SCA91560.1 and SCA91317.1) were identified
132 as potential candidates involved as effectors in cell-to-cell contact growth inhibition. The SCA91317.1
133 protein did not reveal any known functional domains, except for a peptidoglycan-binding lysin (LysM)
134 domain in its N-terminal region. Conversely, the SCA91560.1 protein was predicted to belong to

135 bacterial peptidoglycan hydrolases, harboring a C-terminal Lysozyme-like domain. Given their
136 characteristics, these proteins appear to be potential candidates for the role of cell-to-cell contact
137 growth inhibition effectors in *L. carnosus*. Consequently, SCA91560.1 and SCA91317.1 were
138 designated as LYSO and PLY, respectively.

139 **Gene Expression Analysis of the More Abundant Cell Surface Proteins LYSO and PLY**

140 We determined the transcriptional level of genes encoding LYSO and PLY protein of *L. carnosus* by
141 quantitative reverse-transcription polymerase chain reaction under comparable experimental
142 conditions described above (coculture and monoculture at 25 hours). The transcription levels of *lyzo*
143 and *ply* genes in coculture were quantified as fold changes relative to monoculture, with normalization
144 to the reference *recA* and *rpoB* gene transcription levels. The choice of *recA* for normalization yielded
145 results consistent with those obtained with *rpoB*, as illustrated in the Fig. 2. Similar mRNA expression
146 of *ply* was obtained between the two conditions. However, the transcription level of the *lyzo* gene
147 demonstrated a significant up-regulation (>2-fold) in coculture compared to monoculture, aligning
148 seamlessly with the proteomic data. Consequently, integrating proteomic evidence with subsequent
149 qRT-PCR validation affirmed the overexpression of LYSO protein in *L. carnosus* upon coculture
150 with *L. monocytogenes* cells.

151 **Functional characterization of LYSO protein**

152 The *in silico* analysis predicted that LYSO would encode a protein of 197 amino acids (Fig. 3A) with
153 a deduced molecular mass of 22,230 Da. The N-terminal part of 24 amino acids exhibited all the
154 properties of Gram-positive Sec signal peptide (Sec/SPI) with an identified putative peptidase cleavage
155 site. Furthermore, a transmembrane helix region was predicted between the seventh and the twenty-
156 fourth amino acids. Also, a region of 161 amino acids harboring a Lysozyme_like domain (Pfam

157 PF13702.6) was identified (Fig. 3A). This finding indicates that LYSO is a putative muramidase
158 belonging to the Lyz-like superfamily (cl00222). To examine whether LYSO, possessing a predicted
159 peptidoglycan-degrading activity, could induce the lysis of bacterial cells, toxicity assays were
160 conducted in *Escherichia coli*. We hypothesized that if LYSO is transported in the periplasmic
161 compartment in direct contact with peptidoglycan, it might induce the lysis of *E. coli* cells. To address
162 this inquiry systematically, we employed a cloning strategy to insert the sequence region containing
163 the Lysozyme_like domain of the LYSO gene into two distinct plasmids: pET100 for cytoplasmic
164 expression and pET22b (designated as Peri-LYSO and equipped with the pelB signal peptide) for
165 targeting the protein to the periplasm (Fig. 3B). Subsequently, these recombinant plasmids were
166 introduced into the *E. coli* host. As anticipated for a peptidoglycan-degrading enzyme, the artificial
167 targeting of LYSO to the periplasm through a sec-dependent leader sequence (peri-LYSO) resulted in
168 a significant decrease in *E. coli* viability and optical density. Conversely, the expression of LYSO in
169 the cytoplasm of *E. coli* was notably better tolerated (see Fig. 3C-D). Time-lapse microscopy further
170 revealed that periplasmically localized forms of LYSO proteins (peri-LYSO) induced cell rounding
171 and prompt cell lysis upon induction (Fig. 3E and Supplemental file 2).
172 To assess the cell wall hydrolytic activity of LYSO against *L. monocytogenes*, the recombinant 6-His
173 tagged LYSO protein, lacking the signal peptide (Sec/SPI), was synthesized in *Escherichia coli*
174 Lemo21(DE3) utilizing the pET 100/D-TOPO plasmid. Subsequently, the 6-His tagged protein was
175 purified using NEBExpress Ni Spin Columns. Analysis through SDS-PAGE and Western Blot,
176 employing anti-6xHis tag antibodies, revealed that the purified His-LYSO migrated as a 25 kDa protein
177 (Fig. 4A-B). Afterwards, zymogram gels were employed to assess enzymatic activity, with *L.*
178 *monocytogenes*, *L. carnosus*, or *Micrococcus lysodeikticus* cells serving as substrates. In the
179 zymogram assay using *M. lysodeikticus* cells (suitable substrate for the detection of the bacteriolytic
180 enzyme), distinct clearance bands were observed at 25 kDa and 14 kDa, corresponding to the lytic

181 activity of the purified recombinant LYSO (3µg) and the commercial lysozyme used as a positive
182 control (3µg), respectively (Fig. 4C). Notably, the zymogram experiments demonstrated that the
183 recombinant LYSO also functions as a cell wall hydrolytic enzyme against *L. monocytogenes* (Fig.
184 4D), with no detectable activity observed for *L. carnosus* under the same assay conditions. In summary,
185 these results establish that LYSO exhibits peptidoglycan-degrading enzymatic activity, also targeting
186 *L. monocytogenes* in a zymogram assay.
187 To assess the implication of the LYSO protein in contact-dependent inhibition activity (bacterial
188 antagonism), we conducted coculture assays between wild-type (WT) and Δ*LYSO* strains of *L.*
189 *carnosus* (acting as the "attacker" strain) and *L. monocytogenes* (serving as the "target" strain) (Fig.
190 5A). In the cell-cell contact conditions, *L. carnosus* strains and *L. monocytogenes* were cocultured
191 together in the same well, allowing for extensive and direct cell-cell interactions. This setup
192 substantially reduced the number of recovered target cells (*L. monocytogenes*) compared to non-cell-
193 cell contact conditions, where the attacker and target strains were cocultured in separate compartments
194 using a transwell system as previously. However, the disruption of the LYSO gene led to a significant
195 reduction in inhibitory activity, although it did not altogether abolish it. The number of recovered target
196 cells in contact with the mutant strain increased 10-fold compared to the coculture condition in contact
197 with a wild-type attacker (Fig. 5B). These findings indicate that the LYSO gene plays a role in the
198 observed bacterial antagonism, emphasizing its contribution to the inhibitory effects during direct cell-
199 cell interactions between *L. carnosus* and *L. monocytogenes*.

200 **Discussion**

201 The inhibition observed in LAB with anti-*Listeria* activities suitable for biopreservation generally
202 involves classical mechanisms such as the production of bacteriocins and competition[6]. Recent
203 research has revealed that the *L. carnosus* CNCM I-4031 can prevent the growth of *L. monocytogenes*
204 using a cell-to-cell contact-dependent mechanism[17]. This study provides a comprehensive exploration

205 of the contact-dependent growth inhibition (CDI) mechanism observed in *L. carnosus* CNCM I-4031
206 when interacting with *L. monocytogenes*. Using label-free LC-MS/MS shotgun proteomics and relative
207 gene expression analysis, we identified a key candidate among the cell wall proteins of *L. carnosus*
208 CNCM I-4031: a putative peptidoglycan hydrolase named LYSO. This protein, predicted to be secreted
209 *via* a sec-dependent pathway, contains a Lysozyme-like domain in the C-terminal region and exhibits
210 peptidoglycan hydrolysis activity against *L. monocytogenes*. The knockout mutant of LYSO confirmed
211 its role in CDI. Peptidoglycan hydrolases are a diverse group of enzymes with different origins but
212 similar structural characteristics. They target peptidoglycan, an essential component of bacterial cell
213 walls. By disrupting the cell wall, they cause bacterial cell lysis and play crucial roles in various
214 physiological processes throughout the bacterial life cycle. These enzymes, especially endolysins, are
215 important components of the bacteriophage lytic arsenal. They also play roles in peptidoglycan
216 remodeling and degradation (autolysins) or in competitive interactions among closely related bacterial
217 strains[26,27]. For example, Class III bacteriocins comprise large peptides (Mr ≥ 25 kDa), which are
218 generally heat-labile antimicrobial proteins with enzymatic bactericidal activity targeting the bacterial
219 cell wall. These proteins, known as bacteriolysins, include Enterolysin A, zoocin A, millericin B,
220 bacteriocin 41, stellalysin, and lysostaphin[28–31]. They act by cleaving the peptidoglycan present in the
221 cell walls of sensitive bacteria.

222 Many of bacteriolysins harbor an N-terminal Sec signal sequence and are translated as preproteins to
223 be secreted by the Sec pathway like LYSO protein. The N-terminal Sec signal peptide, which consists
224 of positively charged residues at the N-terminus, a hydrophobic core, and a polar C-terminal cleavable
225 site, is recognized by the Sec-dependent secretion machinery [32]. For example, mature enterolysin A
226 (EnlA) is a class III heat-labile bacteriocin of 316 amino acids, synthesized by *Enterococcus faecalis*
227 as a 343 amino acid preprotein with a Sec-dependent peptide of 27 amino acids. This mature bacteriocin
228 breaks down the cell wall of Gram-positive bacteria, including sensitive *Lactococcus lactis* [31,33].

229 However, contrary to our observations concerning the LYSO killing mechanism, previously studied
230 bacteriolysins from LABs have not been reported to display CDI mechanism. The only previously
231 reported bacteriocin that displays a CDI mechanism in gram-positive bacteria is Listeriolysin S (LLS),
232 a bacteriocin produced by hypervirulent strains of *L. monocytogenes*, which remains localized to the
233 bacterial cell membrane of LLS-producing bacteria and exerts its killing mechanism through direct
234 contact between LLS-producing and target bacteria. This mechanism impairs the membrane integrity
235 of the target bacteria and induces membrane depolarization[24]. These findings underscore the existence
236 of contact-dependent toxin delivery in gram-positive bacteria and emphasize the importance of such
237 interactions in bacterial interspecies competition. In Gram-negative bacteria, contact-dependent
238 inhibition often involves secretion systems, particularly Type IV (T4SS) and Type VI (T6SS) Secretion
239 Systems. These complex molecular machines inject effector proteins, including peptidoglycan
240 hydrolases, into the periplasm of competing bacteria, leading to cell lysis. Such mechanisms facilitate
241 the elimination of rival bacteria through the destruction of their cell walls, highlighting the role of
242 peptidoglycan hydrolases in interbacterial competition[19].

243 The production of antimicrobial molecules, like bacteriocins and T6SS-delivered toxins, is tightly
244 regulated by various cellular mechanisms. In Gram-negative bacteria, T6SS facilitates inter-bacterial
245 antagonism by delivering toxins to neighboring cells, with regulation occurring at pre- and post-
246 translational levels[34]. For instance, in *Pseudomonas aeruginosa*, T6SS assembly is controlled by the
247 kinase PpkA, activated by cell envelope damage from T6SS attacks or other factors[35]. Toxin-specific
248 effectors and signals from quorum sensing and nutrient availability also influence these regulatory
249 processes, enabling bacteria to precisely control toxin production and release for survival and
250 competitiveness[34].

251 The bacteria that produce bacteriocin or deliver toxins directly to target cells through cell-to-cell
252 contact have specific immunity factors that protect the producer strain from being killed by
253 antimicrobial molecules[36]. In our research, we observed that the peptidoglycan of *L. carnosus* is
254 resistant to the lytic activity of LYSO, indicating an inherent self-protection mechanism. This
255 resistance may be due to the structural modifications of the peptidoglycan to reduce the effectiveness
256 of the bacteriolysin. For example, *Staphylococcus simulans* reduces its susceptibility to lysostaphin by
257 by modifying the amino acid composition of interpeptide chains in cell wall peptidoglycan by
258 increasing the serine content and decreasing the glycine content[37]. Accessory cell wall polymers like
259 lipoteichoic acid and teichoic acid also act as endogenous inhibitors of peptidoglycan hydrolases[38].
260 Further research is required to uncover specific self-protection strategies in *L. carnosus*.

261 In summary, our data show that LYSO is a bacteriolytic enzyme involved in countering *L.*
262 *monocytogenes* through *L. carnosus* CNCM I-4031. To our knowledge, it is the first bacteriolysin in
263 gram-positive bacteria known to be implicated in CDI mechanism. Further research is necessary to
264 uncover how LYSO gains access to target cells and how the LYSO-producing cell defends itself from
265 self-toxicity and damage. In addition, further work is needed to decipher the molecular cascade that
266 triggers the expression of LYSO upon contact with target cells. This involves delving into the signaling
267 pathways and regulatory networks that induce LYSO production in response to direct cell-cell
268 interactions. Additionally the role of some genes linked to contact-dependant inhibition and TSS7
269 toxin-antitoxin system evidenced in *L. carnosus* genome[11] in the global inhibition mechanism will have
270 to be elucidated. Understanding these regulatory mechanisms could provide new insights into the
271 adaptive reactions of *L. carnosus* in competitive microbial environments. Future studies should also
272 explore the potential of LYSO as a bacteriolytic agent to control harmful bacteria in the food industry.

273

274 **Methods**

275 **Bacterial strains, culture media, and conditions:**

276 The biopreservative strain of *Lactococcus carnosus* (formerly *L. piscium*) CNCM I-4031 was isolated
277 from fresh salmon steak packed under a modified atmosphere[11]. The food pathogen strain *L.*
278 *monocytogenes* ScottA (CIP 103575) is a clinical isolate purchased from the Collection of Institute
279 Pasteur (CIP). The genome of *L. carnosus* CNCM I-4031 and *L. monocytogenes* ScottA are available
280 in the NCBI genome database under the accession number NZ_FLZT00000000.1 and
281 AFGI00000000.1 respectively [39,40]. The strains were stored at −80 °C in their respective culture media
282 supplemented with 20% glycerol (Sigma Aldrich, Saint-Louis, MO, United States). For precultures, *L.*
283 *carnosus* and *L. monocytogenes* were propagated in Elliker broth (Biokar Diagnostic, Beauvais,
284 France) and Brain heart infusion (BHI) with 2% NaCl (Biokar Diagnostic, Beauvais, France)
285 respectively, for 24 h at 26°C. The bacterial cultures were diluted in their respective fresh medium to
286 obtain appropriate initial cell concentrations when required. *L. monocytogenes* ScottA was enumerated
287 by surface plating on BHI agar supplemented with 2% NaCl after incubation at 37°C for 24h. *L.*
288 *carnosus* CNCM I-4031 cell numbers were estimated by plating on Elliker agar plates incubated at 8°C
289 for 5 days under anaerobic conditions. For monoculture and coculture experiments, the MSMA
290 medium was prepared according to the description of Saraoui *et al.* [17].

291 **Mono and coculture experiments:**

292 Mono and coculture experiments were performed according to the method described by Saraoui *et al*[17].
293 Briefly, coculture and monoculture were achieved in an Erlenmeyer flask containing 400 ml of sterile
294 MSMA medium. *L. carnosus* CNCM I-4031 and *L. monocytogenes* were co-inoculated at
295 10^6 CFU ml^{-1} and 10^3 CFU ml^{-1} in the MSMA medium, respectively. A monoculture of each strain
296 was performed as a control. The flasks were incubated at 26°C for 25 hours, and each experiment was

297 performed in triplicates. The incubation time for cell envelope analysis (25h) represents the time when
298 the growth inhibition of *L. monocytogenes* by *L. carnosus* reaches its maximum[17]. At times 0h and
299 25h, *L. monocytogenes* and *L. carnosus* CNCM I-4031 enumerations were performed as described
300 above to monitor the growth of both strains in different culture conditions and to check the inhibition
301 effect.

302 **Extraction of a fraction enriched in cell envelope proteins**

303 The fractions enriched in cell envelope proteins of coculture and monoculture-grown cells were
304 obtained using a protocol adapted from Gitton *et al.* [41]. Briefly, bacterial pellet was recovered by
305 centrifugation at 12 000 ×g for 5 min at 4°C and resuspended to 80 OD_{600nm} /ml (160mg /mL) in 5ml
306 of Lysis buffer [20 mM sodium phosphate buffer, pH 6.4, 1 X of Protease Inhibitor Cocktail (Sigma-
307 Aldrich), 60 U/mL catalase (Sigma-Aldrich) 10 mM tributylphosphine (Sigma-Aldrich)] maintained
308 at 4°C.

309 After a washing step, the suspended cells were mechanically disturbed with a sonicator (Vibracell
310 72434, Bioblock Scientific, France). The sonications were done using the following parameters: 50W,
311 15 cycles, 15s on/15s off at 4°C. The suspension was centrifuged at 5,000 g for 20 min at 4°C to remove
312 unbroken cells and large cellular debris. The supernatants were collected and subjected to
313 ultracentrifugation at 200 000 g for 30 min at 4 °C to separate the "fraction enriched in cell envelope
314 pellets" from exclusively soluble cytosolic proteins. Finally, the pellets were resuspended in the lysis
315 buffer and sonicated for 15 min at 4 °C in an ultrasonic bath. Protein extracts were prepared for each
316 condition (coculture and monoculture) in three independent experiments. Protein concentration was
317 determined using the Pierce BCA Protein Assay Kit (Thermo Fisher Scientific, France).

318

319 **Gel-based nano–liquid chromatography-tandem mass spectrometry**

320 - **In-gel Digestion and Sample Preparation**

321 Twenty micrograms of resuspended cell-envelope proteins were solubilized in 20 µL of 6% glycerol,
322 50 mM DTT, 2% SDS, 75 mM Tris, pH 6.8, 0.1% bromophenol blue (final concentrations) by
323 sonication for 15 min at 4 °C in an ultrasonic bath. The proteins were then separated by denaturing
324 SDS-PAGE on 4−15% polyacrylamide mini gels (mini-PROTEAN, Bio-rad, France) in 1X of TGS
325 buffer (Bio-rad) with the following parameters: 200 V, 110 mA for 5 min. The gel was stained with
326 Coomassie blue staining (Bio-Safe™ Coomassie, Bio-Rad, France) while shaking on an orbital shaker
327 for 60 min, after which the gel was washed twice with 100 mL of Milli-Q water.

328 The protein band visualized by Coomassie blue staining was excised from the gel, cut into small pieces
329 (≈2 mm slice), and transferred to 1.5-mL microcentrifuge tubes. The gel pieces were rinsed twice with
330 50 mM NH_4HCO_3 and 50% CH_3CN and dried at room temperature. The gel pieces were discolored by
331 washing twice with 50 mM NH_4HCO_3 and 50% CH_3CN and dried at room temperature. The proteins
332 trapped in a gel slice were first reduced in 10mM of DTT at 56°C for 30 min, then they were alkylated
333 using 50 mM of iodoacetamide in the dark for 45 min. The in-gel digestion was performed in 50 mM
334 ammonium bicarbonate pH 8.0, and the quantity of sequencing grade modified trypsin (Promega,
335 sequencing grade) was 0.1 µg per sample. Digestion was carried out at 37°C overnight. The resulting
336 peptides were extracted in several steps: the supernatant of trypsin hydrolysis was transferred to a new
337 tube, and the gel slices were first extracted with the solution of 50 mM CH_3CN, 0.5% Trifluoroacetic
338 acid TFA in water and then using a pure solution of CH_3CN. The gel slices were incubated for 15 min
339 at room temperature for each extraction while shaking. The supernatants of each extraction were pooled
340 with the original trypsin digest supernatant and dried for 1h in a Speed-Vacuum concentrator. The

341 peptides were then resuspended in 15 µL of precolumn loading buffer (0.08% trifluoroacetic acid
342 (TFA) and 2% acetonitrile (ACN in water) before LC-MS/MS analysis.

343 - **LC-MS/MS Analysis**

344 The analysis of digested peptide was performed on an Ultimate 3000 RSLCnano system (Thermo
345 Fisher Scientific, France) coupled to an Orbitrap Fusion Lumos Tribrid Mass Spectrometer (Thermo
346 Fisher Scientific ; PAPPSO proteomic platform, INRA, Jouy-en-Josas). Tryptic peptide mixtures (4µl)
347 were loaded at 20µl/min flow rate onto a desalting precolumn Pepmap C18 (0.3x5mm, 100Å, 5µm,
348 Thermo Fisher Scientific, France). After 4min, the precolumn was connected to the separating
349 nanocolumn Pepmap C18 (0.075x50cm, 100Å, 2µm, Thermo Fisher Scientific, France) and the
350 peptides were eluted with a two-step gradient of buffer B(80 % acetonitrile, 0.1 % formic acid) in
351 buffer A (2 % acetonitrile, 0.1% formic acid) during 65 min. Ionization (1.6 kV ionization potential)
352 and capillary transfer (275°C) were performed with a liquid junction and a capillary probe (SilicaTip™
353 Emitter, 10 µm, New Objective). Peptide ions were analyzed using Xcalibur 3.1.66.10. The machine
354 settings were as follows: 1) full MS scan in Orbitrap (scan range = 400 m/z –1,500 m/z), 2) MS/MS
355 using CID (35% collision energy) in Orbitrap, 3) resolution = 120 000 and 4) fragmentation cycle
356 TopN: Top Speed.

357 - **Processing and Bioinformatics Analyses**

358 The raw files produced under Xcalibur were first converted into mzXML files with MS Convert
359 (ProteoWizard v 3.0.8934). In a second step, protein identification was performed with X!Tandem
360 Piledriver (v 2015.04.01.1) and X! Tandem Pipeline (v 3.4.2 "Elastine Durcie") against a protein
361 database of *L. carnosus* (formerly *L. piscium*) protein database (NCBI, 6937 proteins downloaded
362 March, 13th, 2017) and *L. monocytogenes* (UniprotKB, proteins downloaded March, 13th, 2017), and
363 also against a classical proteomic contaminant database. The X!Tandem search parameters were

364 trypsin specificity with three missed cleavages and variable oxidation states of methionine. Semi-
365 tryptic peptide detection was included by mass tolerance of 10 ppm and a fragment mass tolerance of
366 0.5 Da. The identified proteins were filtered as follows: 1) peptide $E < 0.01$ with a minimum of 2
367 peptides per protein and 2) a protein $E < 10^{-4}$.

368 **Detection of protein abundance changes using Label-free quantification.**

369 After analysis of each independent biological replicate, a final dataset containing only proteins present
370 in all three datasets was generated. Protein abundance was quantified using spectral abundance factor
371 (NSAF) as described before [42,43]. The NSAF for a given protein *k* is defined as follows:

372 $$(NSAF)_k = \frac{(SC/L)_k}{\sum_{i=1}^{N}(SC/L)_i}$$

373 Here, SC represents the number of spectral counts identified for protein *k*, L is the length of protein *k* in
374 amino acid, and the sum is taken over all *N* proteins in the experiment with at least two valid spectral
375 counts out of the three biological experiments. For the statistical analysis of the dataset, the natural log
376 of each NSAF value was calculated, and two-tailed unpaired t-tests were performed to compare the
377 ln(NSAF) from the three biological replicates of the coculture condition against the ln(NSAF) from
378 the three biological replicates of the monoculture condition. Proteins showing differential abundance
379 between the two culture conditions were filtered based on the following criteria: Log2 fold change
380 (NSAF coculture / NSAF monoculture) greater than +2 or less than -2 and *p*-value less than 0.05.
381 Statistical analysis was performed using XLSTAT software (version 2018.4). Statistical analysis was
382 conducted using XLSTAT software (version 2018.4).

383 ***In silico* predictions of protein subcellular localization and function**

384 Prediction of subcellular localization was obtained using the web-server predictors psortb
385 (https://www.psort.org/psortb/)[44]. The molecular function (MF) and biological process (BP)
386 classification of the identified proteins were performed by the Blast2GO software
387 (http://www.blast2go.org/) [45] and BlastKOALA (https://www.kegg.jp/blastkoala/) [46].

388 LYSO amino acid sequence from the *L. carnosus* (formerly *L. piscium)* CNCM I-4031 genome
389 (SCA91560) was analyzed with Interproscan a tool available at the (https://www.ebi.ac.uk/interpro/)
390 and SMART (Simple Modular Architecture Research Tool) is a web resource (http://smart.embl.de/)
391 providing functional analysis and extensive annotation of protein domains and important sites [47,48]. The
392 presence of signal peptides and transmembrane regions was predicted by using SignalP 5.0 server
393 (http://www.cbs.dtu.dk/services/SignalP/index.php) [49].

394 **RNA expression analysis of the differentially expressed cell-surface proteins by RT-qPCR**

395 The cultures were grown in triplicate at 26 °C for 25 h under the conditions previously described.
396 Before RNA isolation, the bacterial samples were directly treated with RNA-protect Bacteria Reagent
397 (Qiagen) to stabilize RNA and were centrifuged at 5000g for 5 min at 4°C to collect the bacterial cells.
398 The bacterial pellets were immediately frozen in liquid nitrogen and stored at -80°C until RNA
399 extraction. The frozen bacterial pellets were subjected to chemical and mechanical disruption using a
400 Lysis buffer (TE 30mM, EDTA 1mM, pH8, Lysozyme 15mg/mL, 20µl Proteinase K) for 10 min at
401 room temperature and a bead beater (FastPrep, Thermo Fisher Scientific) run at a frequency of 5.5 m/s,
402 for 40s, with beads (Matrice de lyse B, MP Biomedicals™,Thermo Fisher Scientific). The total RNA
403 was then extracted using the RNeasy Plant Mini Kit (Qiagen, Germany) according to the
404 manufacturer's instructions. The quality of the obtained RNA was verified by the Nanodrop method
405 and confirmed by electrophoretic analysis on RNA nano. The valid Bacterial RNA was reverse
406 transcribed into cDNA using the iScript™ cDNA synthesis kit (Bio-rad). The expression levels of the

407 two significant MA cell-surface proteins (LYSO and PLY) were examined. The specific primer sets to
408 *L .carnosus* designed for amplification of reference genes (*rpoB* and *recA*) and genes encoding for the
409 MA cell surface proteins are shown in Supplementary Table S2. Relative gene expression was
410 measured by real-time PCR using the SYBR Green Supermix (Bio-rad) and the CFX Real-Time PCR
411 Detection System (Bio-rad). Each experimental group contained two technical replicates. Deionized
412 water was used as a negative control. Relative quantification was performed using the $2^{-\Delta\Delta Ct}$ method,
413 where $\Delta\Delta$ Ct = $(\mathbf{Ct}_{\text{target}} - \mathbf{Ct}_{\text{reference gene}})$ in coculture − $(\mathbf{Ct}_{\text{target}} - \mathbf{Ct}_{\text{reference gene}})$ in monoculture. All
414 the quantifications of target genes were performed in triplicate and were represented as an averaged
415 value ± SD. The difference between the two groups was analyzed using the two-tailed Student *t*-test.
416 $P < 0.05$ was considered significant, with * indicating $P < 0.05$ and ** indicating $P < 0.01$.

417 **Molecular Cloning :**

418 For insertional inactivation of *LYSO* gene, a 461 bp internal fragment of the *LYSO* coding sequence
419 (594 pb) and 1206 bp of erythromycin resistance cassette were amplified by PCR from the
420 chromosomal DNA of *L. carnosus* CNCM-I 4031 and plasmid pHSP02 (Addgene), respectively, using
421 the primer pairs listed in Supplementary Table S2. All PCR products were amplified using Q5® High-
422 Fidelity 2X Master Mix (NEB) and purified using the PCR & DNA Cleanup kit (NEB). Using the
423 Gibson NEB Assembly Kit, the internal fragment and the erythromycin resistance cassette were
424 assembled and ligated into digested puC19 at the EcoRI-HindIII restriction site. Next, the Gibson
425 assembly reaction mixture is transformed into chemically competent *E. coli* DH5α cells. Colony PCR
426 and plasmid miniprep followed by restriction digestion were used to screen for recombinant plasmid
427 containing a desired insert. The insert and the resulting integrative plasmid pUC:emR:*LYSO* were
428 validated by Sequencing at Eurofins Genomics.

429 For recombinant expression, the sequence encoding for truncated *LYSO* protein (residues between 25-
430 197) that lacks the native signal peptide was codon-optimized for *E. coli* using the GeneOptimizer®
431 expert software. The designed sequence gene was synthesized by GeneArt Gene Synthesis Service
432 (ThermoFisher Scientific®) and then was cloned into a pET100/D-TOPO expression vector
433 (ThermoFisher Scientific®), resulting in the expression plasmid pET100::$LYSO_{25\text{-}197}$ (Fig. S5). This
434 expression vector produces N-terminal 6 His-tag $LYSO_{25\text{-}197}$ protein in the cytoplasmic compartment
435 of *E.coli*.

436 For the periplasmic expression vector pET-22b::$LYSO_{25\text{-}197}$, PCR product of 6xHis- LYSO25-197
437 amplified from pET100::$LYSO_{25\text{-}197}$ was subsequently cloned to pET22b (+) (containing the N-terminal
438 pelB sequence) using Gibson assembly (Fig. S6). All primers and plasmids used for cloning are listed
439 in the Supplementary Table S2. The lines of all constructs used in this study were confirmed by DNA
440 sequencing to ensure the absence of point mutations in the cloned genes using the Eurofins Genomics
441 sequencing service.

442 ***E. coli* toxicity assay**

443 For comparison of cytoplasmic versus periplasmic toxicity of LYSO $_{25\text{-}197}$. Overnight cultures of *E.*
444 *coli* Lemo 21 (DE3) carrying empty plasmid (pET-22b or pET100), a plasmid expressing LYSO $_{25\text{-}197}$
445 protein for cytoplasmic (pET100::$LYSO_{25\text{-}197}$) or periplasmic (pET-22-*Peri-LYSO* $_{25\text{-}197}$) localization
446 were adjusted to 1 OD_{600} and serially diluted in LB (1:10) and five µL were spotted onto LB agar
447 (1.5%) containing 100 µg/mL ampicillin with or without 400 µM of IPTG and incubated at 37°C.
448 Images were acquired after 24 hours.

449 For growth curves, overnight cultures of *E. coli* Lemo 21 (DE3) containing empty pET-22b or pET-
450 22b::$LYSO_{25\text{-}197}$ were sub-inoculated to an optical density at 600 nm (OD_{600}) of 0.01 in LB medium
451 supplemented with 100 µg/mL ampicillin and grown at 37 °C. Cultures were induced with 400 µM

452 IPTG after 2h45 of growth. Cell growth was tracked for eight hours by measuring the OD_{600} every 15
453 min. The results represented three independent experiments' mean ± standard deviations (error bars).

454 **Microscopy**

455 For time-lapse microscopy, *E. coli* Lemo 21 (DE3) carrying the pET-22-*Peri-LYSO* $_{25-197}$ plasmid was
456 cultivated in LB medium with ampicillin until reaching an OD_{600} of 0.4-0.5. Five microliters were then
457 placed on 1% LB agar pads supplemented with ampicillin, with or without 400 µM of IPTG. The
458 bacterial growth was observed in a heated chamber at 37°C. Images were captured every 15 minutes
459 for 4 hours using brightfield illumination on a Nikon Ti2 microscope equipped with an ORCA Flash
460 4.0 CMOS camera and an HP APO 1.49 N.A. 100x oil immersion objective. The images were analyzed
461 using NiS-Elements software (version 5.40.01, Nikon Instruments Inc., Nikon Europe B.V.).

462 **Inactivation of the LYSO Gene in *L. carnosus* CNCM-I 4031 by Suicide Vector**

463 The integrative plasmid pUC:em^R:*LYSO* isolated from an *E. coli* 5α transformant was used to transform
464 *L. carnosus* CNCM-I 4031 by electroporation as was essentially done as described before [50,51] with the
465 following modification.

466 *L. carnosus* CNCM-I 4031 colony was inoculated in 5 ml of GM17 (M17 medium containing 0.5%
467 glucose) and cultured at 26°C for eight hours. The preculture was used to inoculate at 1% a G-GM17
468 medium (M17 medium containing 0.5% glucose and 2,5% glycine) and grown at 26°C to an OD600
469 between 0.2 and 0.3. Subsequently, the culture was centrifuged at 6,000 g for 10 min at 4°C, and the
470 collected pellet was washed twice. The cells were first washed with 1 volume ice-cold solution A (0.5
471 M sucrose and 10% glycerol) and centrifuged. Next, The pellet was resuspended in 0.5 volume ice-
472 cold solution A supplemented with 50 mM Na-EDTA, pH 7.5, and incubated for 15 min on ice before
473 centrifugation. Finally, the last wash was done with a 0.25-volume solution. In each step, the pellet

474 was collected by centrifugation at 6,000 x g for 10 min at 4°C and was resuspended by scraping
475 thoroughly. After the last wash, the pellet was resuspended in 0.01 volume ice-cold solution A, and
476 aliquots of 50 µl were flash-frozen with nitrogen? and stored at -80°C until use. For electroporation, a
477 50 µl aliquot of thawed electrocompetent CNCM-I 4031 cells was mixed with 150 ng of
478 pUC:emR:*LYSO* plasmid in an ice-cooled electroporation cuvette (2 mm electrode gap) and exposed
479 to a single electrical pulse of 2 kV field strength, 25 µF capacitance, and 200 Ohm resistance using a
480 Gene Pulser XcellTM (Bio-Rad Laboratories, Richmond, CA, USA). Immediately after discharge, 950
481 µL of ice-cold GM17 containing 20 mM $MgCl_2$ and two mM $CaCl_2$ was added to the cuvette, which
482 was left on ice for 10 min and then incubated at 26°C for 2.5 hours. Finally, transformed cells were
483 plated and fixed for 72 h at 26°C on GM17 medium containing 1.5% agar supplemented with 10 µg·ml-
484 1 erythromycin to select CNCM-I 4031 mutants harboring the inserted pUC:emR:*LYSO*. Vector
485 insertion into the chromosome and disruption of the *LYSO* coding sequence were verified by DNA
486 sequencing of PCR products generated using the primers listed in Supplemental file 2 (for more
487 information, see Fig. S4). In addition, insertion stability was verified after three independent cultures
488 in GM17 and MSMA media without erythromycin. *L. carnosus* WT and Δ*LYSO* growth was monitored
489 in a BHI medium with an initial concentration of 10^6 CFU/ml. 100µL of bacterial suspension was
490 placed in a well of a 96-well plate in triplicate. TECAN monitored growth for 24 hours at 26°C, with
491 $OD_{600\ nm}$ readings taken every 30 minutes.

492 **Bacterial competition experiments**

493 Coculture assays were performed as previously described above with some modifications. The
494 experiments to assess the contact dependence of growth inhibition were done in a Costar six-well
495 polystyrene culture plate (Corning) carrying transwell inserts with a porous membrane (BD Falcon).
496 The membrane contained 0.22 µm pores to restrict the passage and the contact between the inhibitor
497 and target bacteria cells. For coculture without cell-cell interaction, *L. carnosus* (≈10^6 cfu/mL) was

498 added to the transwell insert, and *L. monocytogenes* (≈10^3 cfu/mL) was added to the lower chamber
499 (well). For coculture with cell-to-cell contact, *L. carnosus* (≈10^6 cfu/mL) and *L. monocytogens* (≈10^3
500 cfu/mL) were cultivated in fresh MSMA medium in the same well to allow mixing of both bacteria
501 populations. Plates were covered with a lid and incubated for 25 h at 26 °C. As reported above, viable
502 inhibitor and target cell counts were quantified as colony-forming units per millilitre by plating in
503 selective growth conditions.

504 **Expression and purification of His-tagged LYSO:**

505 The recombinant vector pET100::$LYSO_{25\text{-}197}$ was transformed into *E. coli* Lemo21 (DE3) competent
506 cells (NEB, C2528J) according to manufacturer specifications. The Lemo21 (DE3) cells harbouring
507 the plasmid were grown under agitation (250 rpm) at 37°C in LB medium (Invitrogen, 12780052)
508 containing 100 µg/ml ampicillin and 34 µg/ml chloramphenicol. When bacterial cells reached an
509 OD600 nm of 0.5, 40 µM of IPTG (Thermo scientific®.) was added to induce protein expression.
510 Cultures were induced for approximately 4 hours before being harvested by centrifugation at 6000 rpm
511 for 10 minutes at 4°C and then frozen at -20 °C overnight. The recombinant His-tagged LYSO was
512 expressed in the inclusion bodies (as an insoluble form), and the purification was conducted under
513 denaturing conditions. Briefly, the cell pellets were resuspended in lysis buffer (20 mM sodium
514 phosphate, 300 mM NaCl, 2 mM imidazole, pH 7.4) containing a denaturing agent (8M urea) and were
515 sonicated on ice (12 cycles, 15 sec ON/OFF). The lysed cells were incubated at 25°C for 60 min and
516 then centrifuged at 10,000 rpm for 20 min. The resulting supernatant was subjected to Immobilized
517 metal-affinity chromatography (IMAC) using the Nickel spin column (NEBExpress® Ni Spin
518 columns, NEB). The column was washed three times with Wash Buffer (20 mM sodium phosphate,
519 300 mM NaCl, 20 mM imidazole, 8M urea, pH 7.4). Then, the His-tagged T-LYSO was eluted with
520 the Elution Buffer (20 mM sodium phosphate, 300 mM NaCl, 500 mM imidazole, 8M urea, pH 7.4).
521 The purified protein was quantified using the BCA Protein Assay Kit (Thermo Fisher Scientific,

522 Waltham, MA, USA) according to the manufacturer's instructions. The pure protein was stored at
523 −80°C. The production and the purification of the His-tagged protein were checked by SDS-PAGE and
524 Western blot [52,53], respectively. SDS-PAGE was performed with 12,5% (w/v) polyacrylamide
525 separating gels. Gels were stained with Bio-Safe™ Coomassie Stain solution (Bio-rad). For Western
526 blot assay, the proteins were separated by SDS-PAGE and transferred to nitrocellulose membrane
527 (0,2µm) (Bio-rad) for immunoblot detection with anti-6x-His Tag mouse monoclonal Antibody (HRP)
528 (MA1-21315, Thermo Fisher Scientific) and SuperSignal West Pico PLUS Chemiluminescent
529 Substrate (Thermo Fisher Scientific). Pierce Prestained Protein MW Marker (26612, Life
530 Technologies) and Precision Plus Protein™ Dual Xtra Prestained Protein Standards (1610377, Bio-
531 rad) were used as molecular weight markers.

532 **Zymogram analysis:**

533 The zymogram assay was used to detect cell wall hydrolase activity and was performed as described
534 previously[54] with some modifications. Lytic activity was detected by using SDS–12.5%
535 polyacrylamide gels containing 0.2 % (wt/vol) of *Micrococcus lysodeikticus* cells (M0508, Sigma) or
536 autoclaved cells of *L. carnosus* or *L. monocytogenes.* After sample migration, gels were washed for 15
537 min in deionized H_2O and incubated for 48h at 25°C in Renaturing Buffer (25 mM Tris-HCl, 1% Triton
538 X-10, pH 7,2) to allow for protein renaturation. During this step, the gels were gently shaken with three
539 to five changes of Renaturing Buffer. Subsequently, the gels were washed in deionized H_2O, followed
540 by staining with 0.1% Methylene Blue in 0.01% (w/v) KOH and destained in deionized H_2O. The
541 peptidoglycan hydrolase activity on zymogram gel is identified as a clear band. Commercial lysozyme
542 from hen egg white (Sigma) was used as a positive control for cell wall hydrolase activity. A zymogram
543 assay control was performed in the same way as the normal zymogram, except the protein refolding
544 step was removed [54]. Thus, after the SDS-PAGE was run, the gel was washed and immediately stained
545 with methylene blue solution.

546 **References**

547 1. Guérin, A. *et al.* Advanced 'Omics Approaches Applied to Microbial Food Safety & Quality.
548 in *Food Molecular Microbiology* 88–123 (CRC Press, Boca Raton, FL : CRC Press, 2019. | Series:
549 Food biology series | "A science publishers book.", 2019). doi:10.1201/9781315110110-6.

550 2. Elsser-Gravesen, D. & Elsser-Gravesen, A. Biopreservatives. *Advances in Biochemical*
551 *Engineering/Biotechnology* **143**, 29–49 (2013).

552 3. Camargo, A. C., Todorov, S. D., Chihib, N. E., Drider, D. & Nero, L. A. Lactic Acid Bacteria
553 (LAB) and Their Bacteriocins as Alternative Biotechnological Tools to Control Listeria
554 monocytogenes Biofilms in Food Processing Facilities. *Molecular Biotechnology* **60**, 712–726 (2018).

555 4. Jordan, K. & McAuliffe, O. Listeria monocytogenes in Foods. in *Advances in Food and*
556 *Nutrition Research* vol. 86 181–213 (Academic Press Inc., 2018).

557 5. Borges, F. *et al.* Contribution of omics to biopreservation: Toward food microbiome
558 engineering. *Front. Microbiol.* **13**, (2022).

559 6. Silva, C. C. G., Silva, S. P. M. & Ribeiro, S. C. Application of bacteriocins and protective
560 cultures in dairy food preservation. *Frontiers in Microbiology* **9**, 594–594 (2018).

561 7. Woraprayote, W. *et al.* Bacteriocins from lactic acid bacteria and their applications in meat and
562 meat products. *Meat Science* **120**, 118–132 (2016).

563 8. Gao, Z. *et al.* Inhibitory effect of lactic acid bacteria on foodborne pathogens: A review. *Journal*
564 *of Food Protection* **82**, 441–453 (2019).

565 9. Garcia, E. C. Contact-dependent interbacterial toxins deliver a message. *Current opinion in*
566 *microbiology* **42**, 40–46 (2018).

567 10. García-Bayona, L. & Comstock, L. E. Bacterial antagonism in host-associated microbial
568 communities. *Science* **361**, (2018).

569 11. Werum, V., Ehrmann, M., Vogel, R. & Hilgarth, M. Comparative genome analysis, predicted
570 lifestyle and antimicrobial strategies of *Lactococcus carnosus* and *Lactococcus paracarnosus* isolated
571 from meat. *Microbiological Research* **258**, 126982 (2022).

572 12. Matamoros, S. *et al.* Psychrotrophic lactic acid bacteria used to improve the safety and quality
573 of vacuum-packaged cooked and peeled tropical shrimp and cold-smoked salmon. *Journal of food*
574 *protection* **72**, 365–74 (2009).

575 13. Matamoros, S., Pilet, M. F., Gigout, F., Prévost, H. & Leroi, F. Selection and evaluation of
576 seafood-borne psychrotrophic lactic acid bacteria as inhibitors of pathogenic and spoilage bacteria.
577 *Food Microbiology* **26**, 638–644 (2009).

578 14. Fall, P. A. *et al.* Sensory and physicochemical evolution of tropical cooked peeled shrimp
579 inoculated by Brochothrix thermosphacta and Lactococcus piscium CNCM I-4031 during storage at
580 8°C. *International Journal of Food Microbiology* **152**, 82–90 (2012).

581 15. Fall, P. A., Leroi, F., Chevalier, F., Guérin, C. & Pilet, M.-F. Protective Effect of a Non-
582 Bacteriocinogenic Lactococcus piscium CNCM I-4031 Strain Against Listeria monocytogenes in
583 Sterilized Tropical Cooked Peeled Shrimp. *Journal of Aquatic Food Product Technology* **19**, 84–92
584 (2010).

585 16. Hilgarth, M., Nani, M. & Vogel, R. F. Assertiveness of meat-borne Lactococcus piscium strains
586 and their potential for competitive exclusion of spoilage bacteria in situ and in vitro. *Journal of Applied*
587 *Microbiology* **124**, 1243–1253 (2018).

588 17. Saraoui, T. *et al.* Inhibition mechanism of Listeria monocytogenes by a bioprotective bacteria
589 Lactococcus piscium CNCM I-4031. *Food Microbiology* **53**, 70–78 (2016).

590 18. Chassaing, B. & Cascales, E. Antibacterial Weapons: Targeted Destruction in the Microbiota.
591 *Trends in Microbiology* **26**, 329–338 (2018).

592 19. Russell, A. B., Peterson, S. B. & Mougous, J. D. Type VI secretion system effectors: Poisons
593 with a purpose. *Nature Reviews Microbiology* **12**, 137–148 (2014).

594 20. Souza, D. P. *et al.* Bacterial killing via a type IV secretion system. *Nature Communications* **6**,
595 6453–6453 (2015).

596 21. Willett, J. L. E., Gucinski, G. C., Fatherree, J. P., Low, D. A. & Hayes, C. S. Contact-dependent
597 growth inhibition toxins exploit multiple independent cell-entry pathways. *Proceedings of the National*
598 *Academy of Sciences of the United States of America* **112**, 11341–11346 (2015).

599 22. Jamet, A., Charbit, A. & Nassif, X. Antibacterial Toxins: Gram-Positive Bacteria Strike Back!
600 *Trends in Microbiology* **26**, 89–91 (2018).

601 23. Kobayashi, K. Diverse LXG toxin and antitoxin systems specifically mediate intraspecies
602 competition in Bacillus subtilis biofilms. *PLOS Genetics* **17**, e1009682 (2021).

603 24. Meza-Torres, J. *et al.* Listeriolysin S: A bacteriocin from Listeria monocytogenes that induces
604 membrane permeabilization in a contact-dependent manner. *Proceedings of the National Academy of*
605 *Sciences* **118**, e2108155118 (2021).

606 25. Koskiniemi, S. *et al.* Rhs proteins from diverse bacteria mediate intercellular competition.
607 *Proceedings of the National Academy of Sciences* **110**, 7032–7037 (2013).

608 26. Vollmer, W., Joris, B., Charlier, P. & Foster, S. Bacterial peptidoglycan (murein) hydrolases.
609 *FEMS Microbiology Reviews* **32**, 259–286 (2008).

610 27. Vermassen, A. *et al.* Cell Wall Hydrolases in Bacteria: Insight on the Diversity of Cell Wall
611 Amidases, Glycosidases and Peptidases Toward Peptidoglycan. *Front. Microbiol.* **10**, (2019).

612 28. Simons, A., Alhanout, K. & Duval, R. E. Bacteriocins, Antimicrobial Peptides from Bacterial
613 Origin: Overview of Their Biology and Their Impact against Multidrug-Resistant Bacteria.
614 *Microorganisms* **8**, 639 (2020).

615 29. Bastos, M. do C. de F., Coutinho, B. G. & Coelho, M. L. V. Lysostaphin: A Staphylococcal
616 Bacteriolysin with Potential Clinical Applications. *Pharmaceuticals* **3**, 1139–1161 (2010).

617 30. Lahiri, D. *et al.* Bacteriocin: A natural approach for food safety and food security. *Front.*
618 *Bioeng. Biotechnol.* **10**, (2022).

619 31. Nilsen, T., Nes, I. F. & Holo, H. Enterolysin A, a Cell Wall-Degrading Bacteriocin from
620 Enterococcus faecalis LMG 2333. *Applied and Environmental Microbiology* **69**, 2975–2984 (2003).

621 32. Kurushima, J., Hayashi, I., Sugai, M. & Tomita, H. Bacteriocin Protein BacL1 of Enterococcus
622 faecalis Is a Peptidoglycan d-Isoglutamyl-l-lysine Endopeptidase*. *Journal of Biological Chemistry*
623 **288**, 36915–36925 (2013).

624 33. Hickey, R. M., Twomey, D. P., Ross, R. P. & Hill, C. Production of enterolysin A by a raw
625 milk enterococcal isolate exhibiting multiple virulence factors. *Microbiology (Reading)* **149**, 655–664
626 (2003).

627 34. Alcock, F. & Palmer, T. Activation of a bacterial killing machine. *PLoS Genet* **17**, e1009261
628 (2021).

629 35. Basler, M., Ho, B. T. & Mekalanos, J. J. Tit-for-Tat: Type VI Secretion System Counterattack
630 during Bacterial Cell-Cell Interactions. *Cell* **152**, 884–894 (2013).

631 36. Kennedy, N. W. & Comstock, L. E. Mechanisms of bacterial immunity, protection, and survival
632 during interbacterial warfare. *Cell Host & Microbe* **32**, 794–803 (2024).

633 37. DeHart, H. P., Heath, H. E., Heath, L. S., LeBlanc, P. A. & Sloan, G. L. The lysostaphin
634 endopeptidase resistance gene (epr) specifies modification of peptidoglycan cross bridges in
635 Staphylococcus simulans and Staphylococcus aureus. *Appl Environ Microbiol* **61**, 1475–1479 (1995).

636 38. Beukes, M. & Hastings, J. W. Self-Protection against Cell Wall Hydrolysis inStreptococcus
637 milleri NMSCC 061 and Analysis of the Millericin B Operon. *Applied and Environmental*
638 *Microbiology* **67**, 3888–3896 (2001).

639 39. Briers, Y., Klumpp, J., Schuppler, M. & Loessner, M. J. Genome sequence of Listeria
640 monocytogenes Scott A, a clinical isolate from a food-borne listeriosis outbreak. *Journal of*
641 *Bacteriology* vol. 193 4284–4285 Preprint at https://doi.org/10.1128/JB.05328-11 (2011).

642 40. Marché, L. *et al.* Complete genome sequence of Lactococcus piscium CNCM I-4031, a
643 bioprotective strain for seafood products. *Genome Announcements* **5**, (2017).

644 41. Gitton, C. *et al.* Proteomic signature of Lactococcus lactis NCDO763 cultivated in milk.
645 *Applied and Environmental Microbiology* **71**, 7152–7163 (2005).

646 42. Zybailov, B. *et al.* Statistical Analysis of Membrane Proteome Expression Changes in
647 Saccharomyces cerevisiae. *J. Proteome Res.* **5**, 2339–2347 (2006).

648 43. Paoletti, A. C. *et al.* Quantitative proteomic analysis of distinct mammalian Mediator
649 complexes using normalized spectral abundance factors. *Proc Natl Acad Sci U S A* **103**, 18928–18933
650 (2006).

651 44. Yu, N. Y. *et al.* PSORTb 3.0: improved protein subcellular localization prediction with refined
652 localization subcategories and predictive capabilities for all prokaryotes. *Bioinformatics* **26**, 1608–
653 1615 (2010).

654 45. Conesa, A. *et al.* Blast2GO: A universal tool for annotation, visualization and analysis in
655 functional genomics research. *Bioinformatics* **21**, 3674–3676 (2005).

656 46. Kanehisa, M., Sato, Y. & Morishima, K. BlastKOALA and GhostKOALA: KEGG Tools for
657 Functional Characterization of Genome and Metagenome Sequences. *Journal of Molecular Biology*
658 **428**, 726–731 (2016).

659 47. Mitchell, A. *et al.* The InterPro protein families database: the classification resource after 15
660 years. *Nucleic Acids Research* **43**, D213–D221 (2015).

661 48. Letunic, I. & Bork, P. 20 years of the SMART protein domain annotation resource. *Nucleic*
662 *Acids Research* **46**, D493–D496 (2018).

663 49. Almagro Armenteros, J. J. *et al.* SignalP 5.0 improves signal peptide predictions using deep
664 neural networks. *Nature Biotechnology* **37**, 420–423 (2019).

665 50. H, H. & If, N. High-Frequency Transformation, by Electroporation, of Lactococcus lactis
666 subsp. cremoris Grown with Glycine in Osmotically Stabilized Media. *Applied and environmental*
667 *microbiology* **55**, (1989).

668 51. Wells, J. M., Wilson, P. W. & Le Page, R. W. Improved cloning vectors and transformation
669 procedure for Lactococcus lactis. *J Appl Bacteriol* **74**, 629–636 (1993).

670 52. Laemmli, U. K. Cleavage of structural proteins during the assembly of the head of
671 bacteriophage T4. *Nature* **227**, 680–685 (1970).

672 53. Towbin, H., Staehelin, T. & Gordon, J. Electrophoretic transfer of proteins from
673 polyacrylamide gels to nitrocellulose sheets: Procedure and some applications. *Proceedings of the*
674 *National Academy of Sciences of the United States of America* **76**, 4350–4354 (1979).

675 54. Escobar, C. A. & Cross, T. A. False positives in using the zymogram assay for identification of
676 peptidoglycan hydrolases. *Anal Biochem* **543**, 162–166 (2018).

677

Acknowledgements (not compulsory)

This work was financially supported by the COM-BACT and PULSAR LYSO projects, funded by the Région des Pays de la Loire, France. The authors thank Monique Zagorec and Christine Delbarre-Ladrat for their assistance in conceptualization, and Hakima Lakhal and Ombeline Guiguin for their contributions to the experimental work. They also thank Biogenouest, the Western France network of life sciences and environmental technology core facilities supported by the Conseil Régional des Pays de la Loire, for their support of APEX.

Author contributions statement

MFP, FL, and JB supervised the project. RT, MFP, DP, and FL contributed to conceptualization. RT, MFP, SR, MH, HL, and OG conducted the experiments. LD supervised and analyzed the microscopic experiments, and VM supervised the proteomic experiments. RT, SR, and MFP analyzed the results. RT and MFP wrote the manuscript. All authors reviewed the manuscript.

Competing interest

The author(s) declare no competing interests.

Data availability

All data generated or analyzed during this study are included in this published article and its supplementary information files.

698 **Main Figures**

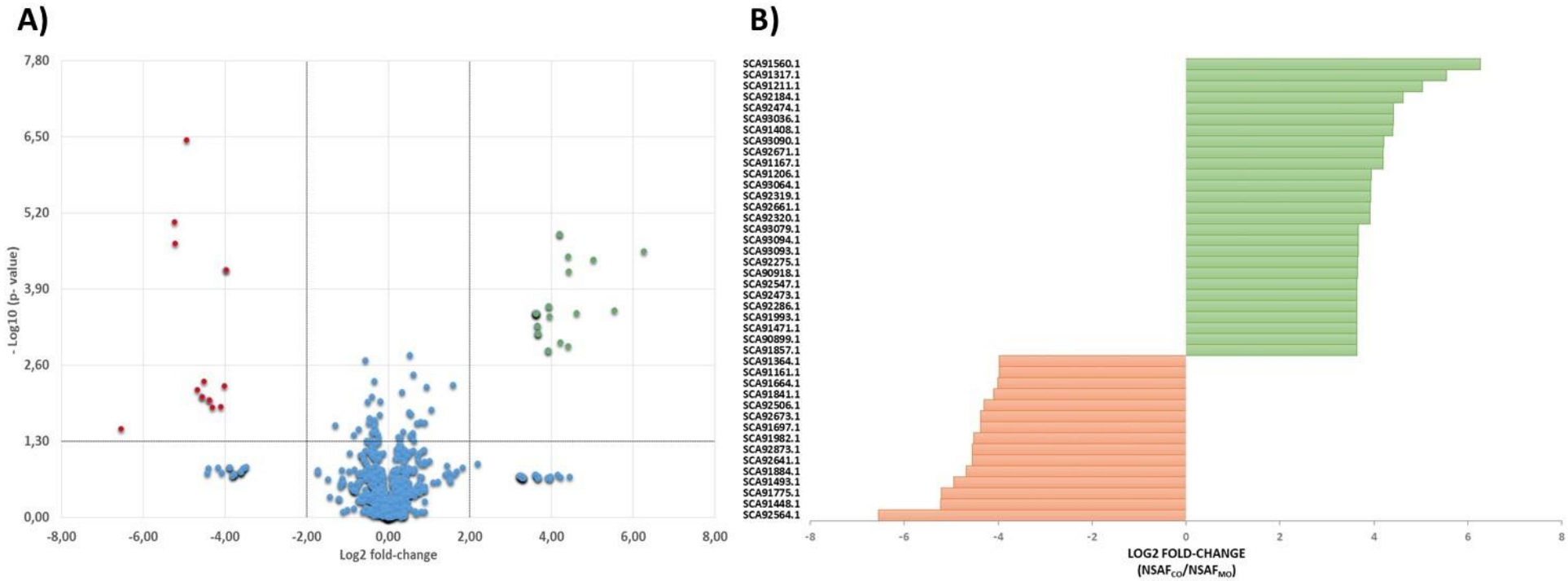

699

700 **Figure 1. Label-free proteomics analysis of *L. carnosus* CNCM I-4031 in coculture and monoculture.** (a) Volcano plot of differentially
701 abundant proteins (t-test $p \leq 0.05$ and log2 fold change cutoff point ±2) between the coculture and the monoculture condition. Y-axis indicates
702 – Log10 (*p*-value), X-axis shows *L. carnosus* protein abundance ratio in Coculture (CO) vs monoculture (MO). The color code indicates more
703 abundant proteins (green) and low abundant proteins (red). Proteins with no statistically significant difference in abundance between the two
704 conditions are shown in blue. (b) The bar chart shows the mean log2 (fold change NSAF coculture/NSAF monoculture) of the proteins
705 abundance of *L. carnosus*. The positive fold changes (green) and the negative fold changes (red), indicate respectively the more abundant
706 (MA) proteins and the less abundant (LA) proteins observed in the coculture condition.

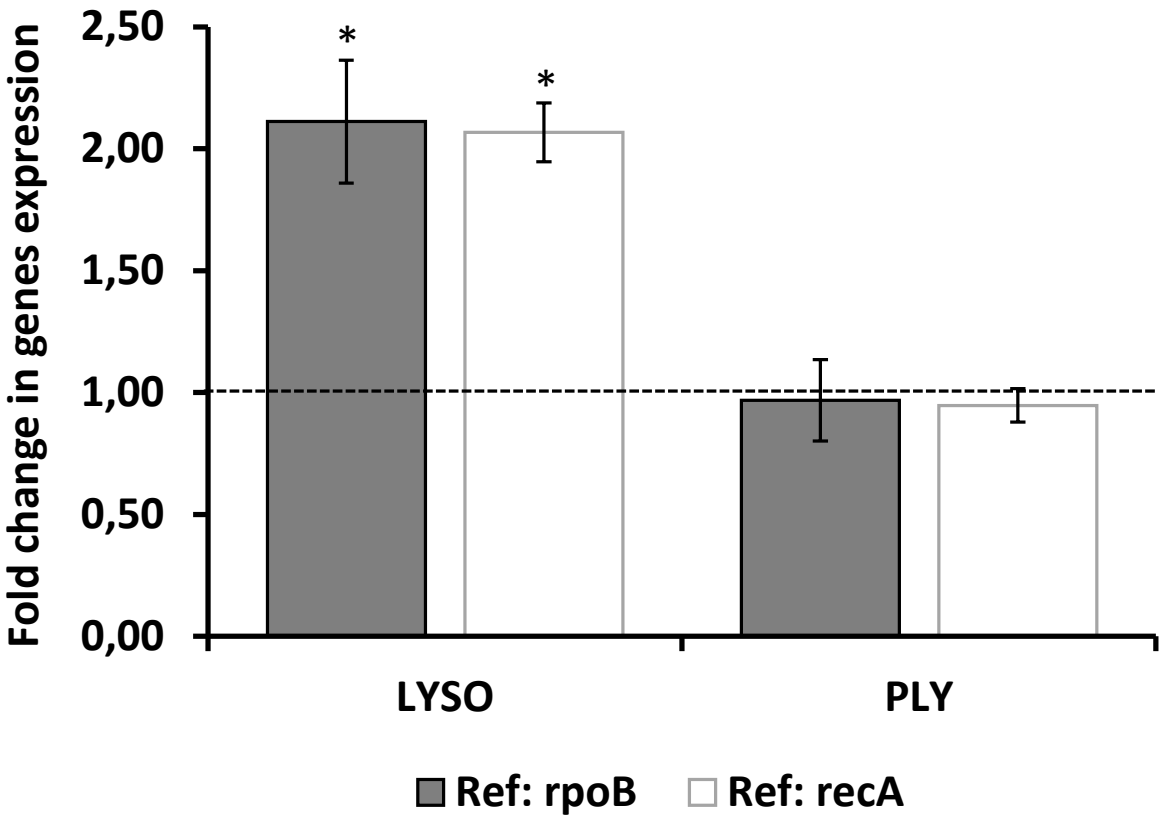

707

708

709 **Figure 2. Effect of coculture with *L. monocytogenes* Scott A on the expression of *L. carnosus* CNCM I-4031 LYSO and PLY encoding**
710 **genes.** The coculture and monoculture of ***L. carnosus*** CNCM I-4031 were conducted in MSMA broth at 26°C for 25h. Fold change in mRNA
711 expression of target genes was determined using Real-Time Quantitative PCR and the $2^{-\Delta\Delta CT}$ Method. Growth of the CNCM I-4031 strain in
712 monoculture was used as a control. Expression levels were normalized against the reference genes *rpoB* and *recA*. Error bars represent SD
713 from three replicates and * $p < 0.05$.

714

715

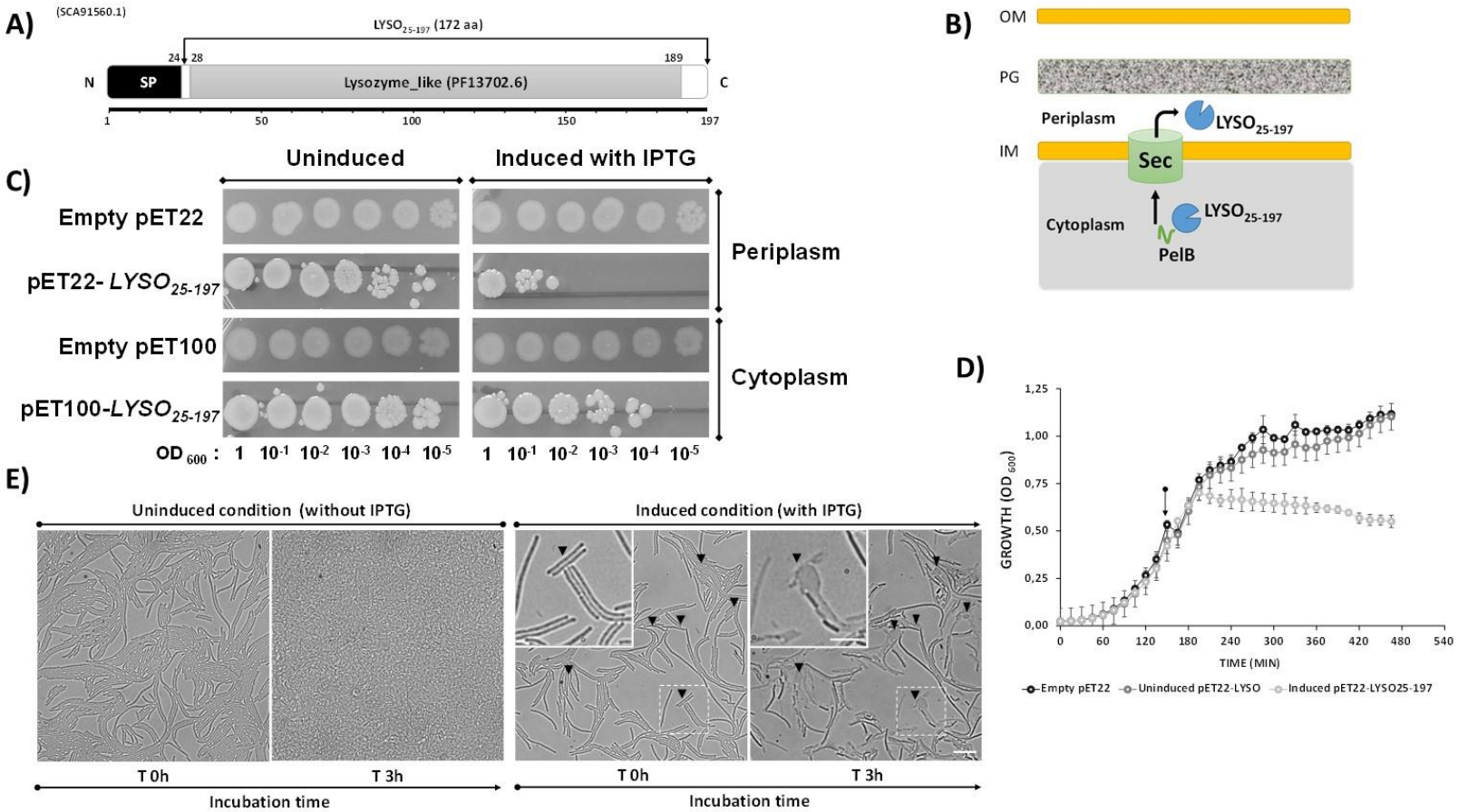

716

717 **Figure 3. Directed export of LYSO$_{25\text{-}197}$ protein to the periplasm of *E. coli* is toxic and results in cell lysis.** (**A**) Schematic of the domain
718 and motif organization of the LYSO protein (SCA91560.1). The black box indicates the signal peptide (SP) located within the protein's N-
719 terminal amino acids 1 to 24. The gray box indicates 161 amino acids of the Lysozyme_like domain (Pfam PF13702.6). Domains, motifs, and
720 amino acid positions were assigned with Interproscan, SMART, and SignalP 5.0. Numbers indicate the amino acid positions. The indicated
721 172 amino acid represents the segment expressed in *E. coli* (From the 25th to the 197th aa). **(B)** Schematic representation of the toxicity
722 experiments in (C). IM, inner membrane; OM, outer membrane; PG, peptidoglycan; PelB, signal peptide. **(C)** Gene encoding *L. carnosus*
723 CNCM I-4031 LYSO protein was heterologously expressed in the cytoplasm or periplasm compartment of *E. coli* Lemo21(DE3) using pET100

724 or pET22 plasmid, respectively. For pET22, periplasmic localization was achieved by fusion the PelB leader sequence at the N-terminus of
725 the LYSO protein. Serial dilutions of *E. coli* strains were spotted on LB media plates, and gene expression was induced with IPTG. The used
726 vectors are indicated on the left, and the density of the inoculum is given at the bottom of the images. The empty vectors were used as a
727 negative control. Plates were incubated at 37 °C for 18 h, after which they were photographed. **(D)** Growth curves of *E. coli* Lemo21(DE3)
728 harboring indicated plasmids were obtained by measuring OD_{600} at 15 min intervals. Cultures were induced at the indicated time (arrow) with
729 IPTG. Error bars indicate ± s.d. (n = 3). **(E)** Representative micrographs of *E. coli* Lemo21(DE3) harboring pET22-$LYSO_{25-197}$ grown on LB
730 agar pads in uninduced (without IPTG) or induced condition (with IPTG). After spotting cells on LB agar pads, the frames were acquired at T
731 0h and T 3h. Arrowhead indicated strains before (T0) and after lysis (T3h) in the presence of IPTG. Scale bar 10µm (original size). Scale bar
732 5 µm (inset area – dotted white).

733

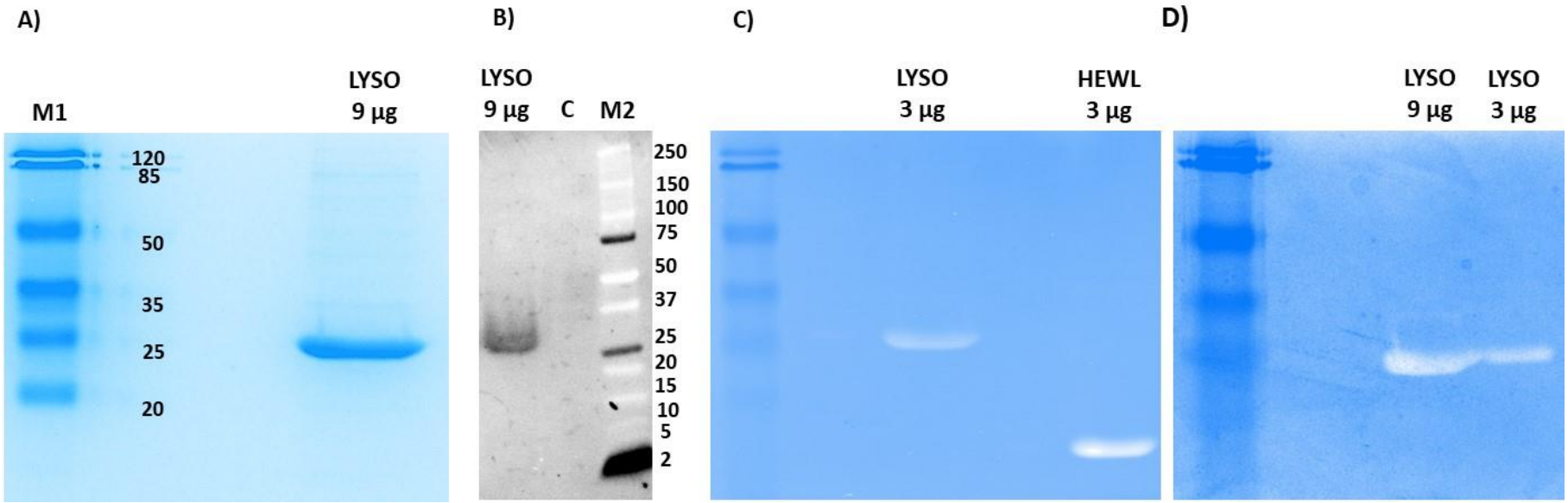

Figure 4. The lytic activity detection of LYSO protein against *Micrococcus lysodeikticus* and *Listeria moncytogenes* cell walls. (A) SDS-PAGE and (B) Western blot analysis showing 6x-His-tagged $LYSO_{25-197}$ protein used for the zymogram assay after purification using NEBExpress Ni Spin Columns. A 25 kDa band corresponding to the recombinant 6x-His-tagged $_{LYSO25-197}$ was observed. The gel electrophoreses were conducted using 12.5% SDS-PAGE gel. Western blot analysis was performed by loading the negative control C and nine µg of the 6x-His-tagged $LYSO_{25-197}$. The resolved proteins were transferred onto nitrocellulose and probed with Anti-6x-His Tag Mouse Monoclonal Antibody (MA1-21315-HRP) for the western blot. Chemiluminescent detection was performed using SuperSignalWest Pico PLUS Chemiluminescent Substrate (34577). Protein markers: M1, Pierce Prestained Protein MW Marker (26612, Life Technologies) and M2, Precision Plus Protein™ Dual Xtra Prestained. Zymogram analysis of peptidoglycan hydrolase activity of the purified 6x-His-tagged $LYSO_{25-197}$ protein against (C) *Micrococcus lysodeikticus* and (D) *Listeria moncytogenes* ScottA. The Hen Egg-White Lysozyme (HEWL) lysozyme is included as a positive control. The zymogram gels contained 0.2 % (wt/vol) of autoclaved *Listeria monocytogenes* cells or *Micrococcus lysodeikticus* cells (M0508, Sigma) as substrate. The amount of each protein loaded onto the gel is shown in micrograms at the top of the figure.

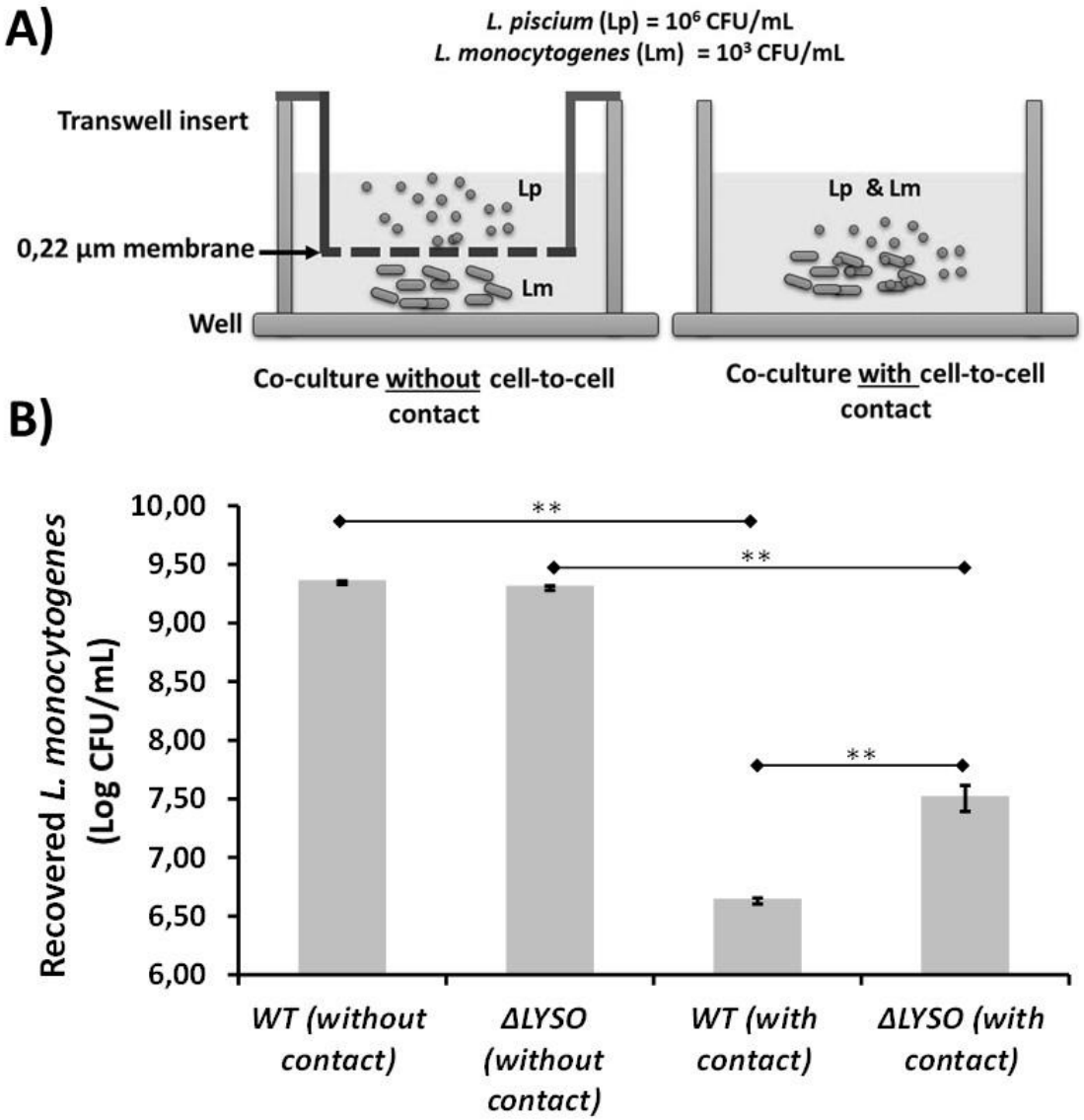

Figure 5. LYSO protein plays a role in the contact-dependent inhibition activity of *L. carnosus* against *L. monocytogenes*. (B) Recovery of viable *Listeria monocytogenes* ScottA following coculture with the CNCM I-4031 wild-type strain (WT) or the isogenic *ΔLYSO* strain. Data are presented as the mean ± SD of three independent experiments. The P-values were determined using a two-tailed unpaired Student's t-test, and differences were acknowledged as statistically significant at $P < 0.05$. (A) The experimental setup of the competition assays. Two different modes of coculture system were used. In non-cell-to-cell contact conditions, *L. carnosus* and *L. monocytogenes* Scott A cells were cocultured in two different compartments (insert membrane and well). The medium is shared between the inner and outer compartments, while the cells cannot pass the 0.22 µm membrane barrier. In cell-cell contact conditions, both cells are mixed and cultured on the same well, thus allowing extensive and direct cell-cell interactions. The competition assays were done on the MSMA medium at 26°C for 25h. Each strain's initial and final populations were enumerated by plating on selective culture conditions.

763 **Main Table(s)**

764 **Table 1.** Subcellular distribution and biological process classification of the more abundant (MA)
765 proteins in the coculture condition.

ID	Description	Biological process	Molecular function	Cellular destination
SCA91471.1	Conserved hypothetical protein		Unk	Unk
SCA93036.1	Conserved hypothetical protein		Unk	Unk
SCA91317.1	Putative lysozyme or peptidoglycan lyase containing peptidoglycan-binding lysin domain	Unk	LysM domain	Surf
SCA91560.1	Lytic murein transglycosylase family (Lysozyme like)		Lysozyme-like [E:C:3.2.1.14; EC:3.2.1.17]	Surf
SCA92671.1	Putative transcriptional regulator	Regulation of DNA-templated transcription	DNA binding	Cyto
SCA92286.1	putative transcriptional regulator, LysR family		DNA binding; DNA-binding transcription factor activity	Cyto
SCA92661.1	Putative transcriptional regulator		DNA binding	Cyto
SCA93079.1	Ribose operon repressor		DNA binding	Cyto
SCA93090.1	Putative bacterial Mobilization protein mobC	Plasmid replication & mobilization	MobC-like: belong to the group of relaxases	Unk
SCA93093.1	Adenosine monophosphate-protein transferase, fic (filamentation induced by cAMP)domain		AMPylase activity	Cyto
SCA93094.1	Putative replication initiator protein, RepB		DNA-directed DNA polymerase activity	Cyto
SCA92319.1	N5-carboxyaminoimidazole ribonucleotide mutase	Purine transport & metabolism	Isomerase activity; purE; [EC:5.4.99.18]	Cyto
SCA91857.1	Phosphoribosylaminoimidazole synthetase		Phosphoribosylformylglycinamidine cyclo-ligase activity; purM; [EC:6.3.3.1]	Cyto
SCA92320.1	Phosphoribosylamine--glycine ligase		Phosphoribosylamine-glycine ligase activity; ATP binding; metal ion binding; [EC:6.3.4.13]	Cyto
SCA90899.1	Phosphatidate cytidylyltransferase (CDP-diglyceride synthase)	Lipid transport & metabolism	Transferase activity, transferring phosphorus-containing groups; [EC:2.7.7.41]	Memb
SCA90918.1	Putative Glycerophosphoryl diester phosphodiesterase (GLPQ, YQIK)		Phosphoric diester hydrolase activity; [EC:3.1.4.46]	Cyto
SCA91408.1	Putative 3-oxoacyl-acyl carrier protein reductase		Oxidoreductase activity; fabG; [EC:1.1.1.100]	Cyto
SCA91167.1	Holliday junction resolvase	DNA recombination & repair	Nuclease activity; ruvX; [EC:3.1.-.-]	Cyto
SCA91206.1	Holliday junction ATP-dependent DNA helicase RuvA		DNA helicase activity; ATP binding; four-way junction helicase activity; DNA binding; ruvA [EC:3.6.4.12]	Cyto
SCA91211.1	ATP-dependent DNA helicase, component of RuvABC resolvasome		ATP binding; DNA binding; four-way junction helicase activity; ATP hydrolysis activity; ruvB; [EC:3.6.4.12]	Cyto
SCA92474.1	PTS system, trehalose-specific IIB component	Carbohydrate transport & metabolism	Trehalose transmembrane transporter activity; [EC:2.7.1.201]	Memb
SCA92473.1	Trehalose-6-P hydrolase / GH13, similar to LACPI-1657 from L. piscium MKFS47		Alpha,alpha-phosphotrehalase activity; treC; [EC:3.2.1.93]	Cyto
SCA92275.1	Glucan 1,6-alpha-glucosidase / GH13, similar to LACPI-1446 from L. piscium MKFS47		Alpha-amylase activity; Dextran glucosidase; [EC:3.2.1.70]	Cyto
SCA92547.1	Glutamate and aspartate transporter subunit; ATP-binding component of ABC superfamily	Amino acid transport & metabolism	ATP binding; ATP hydrolysis activity; ABC-type amino acid transporter activity; ABC.GLN1.A; [EC:3.6.3.-]	Memb
SCA91993.1	Glutamate racemase		Glutamate racemase activity; murI; [EC:5.1.1.3]	Cyto
SCA92184.1	Arginine biosynthesis bifunctional protein ArgJ		Glutamate N-acetyltransferase activity; [EC:2.3.1.35, EC:2.3.1.1]	Cyto
SCA93064.1	Imidazoleglycerol-phosphate dehydratase		imidazoleglycerol-phosphate dehydratase activity; hisB; [EC:4.2.1.19]	Cyto

766

767 **Unk :** Unknown, **Surf :** Surfaceome, **Memb :** Membranome, **Cyto :** Cytoplasmic.

Supplementary Files

This is a list of supplementary files associated with this preprint. Click to download.

- Supplementalfile1TotalproteinsScientificReports.xlsx
- Supplementalfile2TimelapseScientificReports.zip
- SupplementaryInformationScientificReports.pdf